

Diesel Engine Control Strategy for a Programmable Engine Control Unit *

Mario Farrugia, Charlo Seychell, Stephen Camilleri, Gilbert Farrugia, Carl Caruana, and Michael Farrugia

Abstract— Diesel engines are controlled with Engine Control Unit (ECU) to provide flexibility on injection schemes mostly in support of lower emission targets. Research on diesel engines requires programmable ECU to allow experimental investigation of the effects of varying diesel injection and other parameters such as Exhaust Gas Recirculation (EGR). The development of a programmable ECU for common rail diesel engines is discussed in this paper. The control strategy used in the programmable ECU is detailed. Experimental data on flowrates of the solenoid type diesel injectors is given and discussed. Experimental performance data from the loaded engine controlled with the programmable ECU and using the outlined strategy is also given and discussed. The tested control scheme is an extension to the control scheme typically used on gasoline engine, also known as speed-density control. The ECU is also a development on a programmable gasoline ECU with the addition of an external power module.

Keywords— electronic engine control; diesel engine control; speed-density control; peak and hold injectors; compression ignition, torque requirement input.

I. INTRODUCTION

Automotive system are a well known and accepted application of electronic control not only for engines but also on the drivability aspect [1]. ECU evolution through the years has been motivated by emission control and took advantage of the ever growing electronic capabilities. Hagen [2] and Brietzman [3] report the early ECU advancements at Ford in the 70's. While from Bosch, Gerhardt [4] report that electronic systems started with a simple injection system with a separate ignition unit in the early 70's, and then injection and ignition were integrated into one single electronic control unit during the 80's. Look-up tables were and are still widely used in engine management strategies to characterize nonlinear relationships between inputs and the desired output [5].

The general concept of the ECU functionality and key timing requirements and calculation periods within the cycle are still as explained by Breitzman [3]. However new features such as use of Field Programmable Gate Array (FPGA) or Application Specific Integrated Circuits (ASIC) today greatly enhances the ECU capabilities [6][7][8].

*Research supported by University of Malta.

Mario Farrugia is with University of Malta; e-mail: mario.a.farrugia@um.edu.mt

Charlo Seychell, Stephen Camilleri, Gilbert Farrugia and Carl Caruana were with University of Malta.

Michael Farrugia is with Reata Engineering, www.reataengineering.com

Axelsson [8] discusses how the use of ASIC gives the possibility of shifting the partitioning between HardWare and SoftWare. Other ECU advancements relate to connectivity such CAN, OBD, Bluetooth and also Android applications [9].

Research into alternative fuels led many researchers to require the use of non OEM ECUs and revert to programmable and configurable ECUs. Sáinz [10] used a commercially available programmable ECU for their work on conversion of a carbureted single cylinder electric generator engine to bi-fuel, hydrogen and gasoline. The conversion required the installation of sensors as required by the used aftermarket ECU (DTAfast®). On the other hand Oliviera [11] built a specific ECU based on three Freescale microcontrollers to supplement hydrogen in the inlet of a 4 cylinder electric generator diesel engine. The ECU architecture is discussed and details of the ECU electronics is given. A PLC based ECU was implemented by Ergenç [12] for a dual fuel application, diesel and LPG. This was possible due to the real-time operating system, counters and timers of the Siemens PLC used. The reported work was on a single cylinder conventional, *i.e.* mechanical fuel injection, converted to diesel electronic fuel injection and supplemental port fuel injection of LPG. Wierzbicki [13] also converted the original mechanical fuel injection system on a Yanmar single cylinder diesel engine to electronic injection system but opted for a Drivven® system by National Instruments for the study of mixing a synthesized biogas with diesel fuel. Investigations of diesel blends with n-butanol and isobutanol was reported by Xiaolei Gu [14] who used Etas Inca to do calibration changes of injection timing and EGR rates on a Ford Lion V6 engine.

The use of non OEM ECU is required to test control schemes such as reported by Tschanz [15] who implemented PM and NOx feedback control study by using an Etas rapid prototyping system for the calibration experiments on a 6 cylinder 3 liter Daimler diesel engine. Unconventional engines can also lead to non standard ECU such as the work in progress using Arduino reported by Giordani [16] to control an unconventional rotary SI engine.

Elaborate control schemes can be implemented to manage engines but these might be too complex for simple ECU's [17]. In general the testing of control schemes requires use of programmable ECU as done by Wong [18] who used a Motec® to test AFR predictive learning on a performance vehicle. Performance and racing applications also now entail the use of programmable ECU as outlined by Hiticas [19] to control a turbocharged SI engine.

II. DEVELOPMENT OF THE REATA ECU

The ECU development was initially targeted for naturally aspirated gasoline engine as detailed in Farrugia [20]. Subsequently the same ECU was used for more complex configurations of the gasoline engine namely, turbocharging[21], hydrogen enhanced combustion [22], water injection [23][24]and also Liquefied Petroleum Gas (LPG) in liquid state [25].

The general outline of the ECU hardware is shown in Figure 1. It uses a 16 bit Freescale microcontroller MC9S12XDP512, clocked at a frequency of 16MHz. This micro controller has a second controller core termed XGATE. The XGATE is used to read the sensors connected to the ADC and filter the signals. The software for the microcontroller was written in ANSI C and assembly language, using the Code Warrior compiler and IDE from Freescale.

A Graphical User Interface (GUI) was developed to provide real time control of the desired engine parameters. The GUI runs on PC and was written in C++ using Visual Studio from Microsoft. Additionally an Android application was written to provide additional information to the driver as an extension to the dashboard. It also provides for ON/OFF switching of outputs, again intended as an extension of the dashboard. Further details of the ECU are given in Farrugia [26].

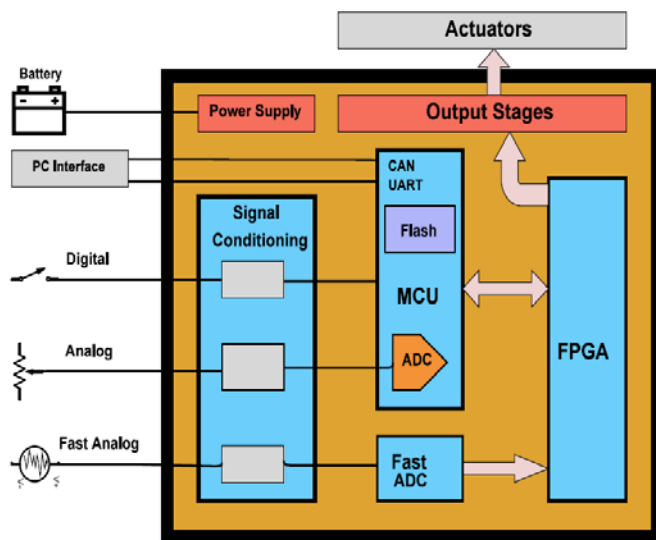


Figure 1. ECU architecture

III. DIESEL INJECTOR POWER MODULE

The adaption to control a common rail diesel engine is detailed in this section. The diesel engine used in this work is a Peugeot 2.0 liter HDi engine, year of production 2000. The Spark Ignition ECU main features to control fuel quantity and spark timing were used to control diesel fuel injection

duration and diesel injection timing respectively. However, while in SI fuel duration and ignition timing are on different outputs, in CI, both duration and timing are required on the same output *i.e.* on the diesel injection pulse. One major limitation adopted in this work to keep the project manageable was the use of main injection only, *i.e.* no pilot injections were implemented. The implementation of pilot injection would need a diversified embedded software and GUI that would have to be completely separate project from the gasoline ECU.

A. Voltage Requirement for Diesel Injector Power Switching

The electrically operated injectors are discussed in Bosch [27](pg 282-283). The different phases of injector opening, pickup current phase, holding-current phase and switch-off are discussed. Values of pickup current are stated to be approximately 20A, while the boost voltage to generate a steep current rise is stated to be up to 50V.

For an inductor and series resistor connected to a constant voltage supply, transient current flow is given by equation 1.

$$i = \frac{V}{R}(1 - e^{-Rt/L}) \quad (1)$$

This was used to establish/confirm the order of voltage that needs to be applied to the diesel injector to reach the 20 amp threshold current in a time of the order of 0.1ms. The electrical resistance and inductance of the Bosch diesel injector used on the Peugeot 2.0 liter HDi series engine is given in table 1. The table also lists other gasoline injector variants for comparison. Figure 2 shows the current increase in the three different types of injectors to show the relative difference in current rise due to the different injectors inductance and internal resistances. The three injectors are a typical saturation 250cc/minute gasoline high impedance injector; a low impedance 1200 cc/minute gasoline injector; and the Peugeot Bosch common rail diesel solenoid valve injectors used in this study.

TABLE I. INJECTOR INDUCTANCE AND RESISTANCE

Injector	Inductance mH	Internal Resistance Ω
Gasoline high impedance 250cc/min injector	7.35	14.37
Gasoline low impedance 1200cc/min injector	3.39	2.21
Diesel Bosch solenoid type injector	0.19	0.41

Figure 2 shows that for the diesel common rail injector a voltage quite higher than the typically available 12 V in an automotive setup is required to increase the current to a substantial value of 20Amp in a relatively short time such as 0.1ms. This is generally in conformance with statements in Bosch [27], however this electrical analysis shows that a value of 70 V (rather than 50V mentioned in [27]) is better for an adequate fast current rise time.

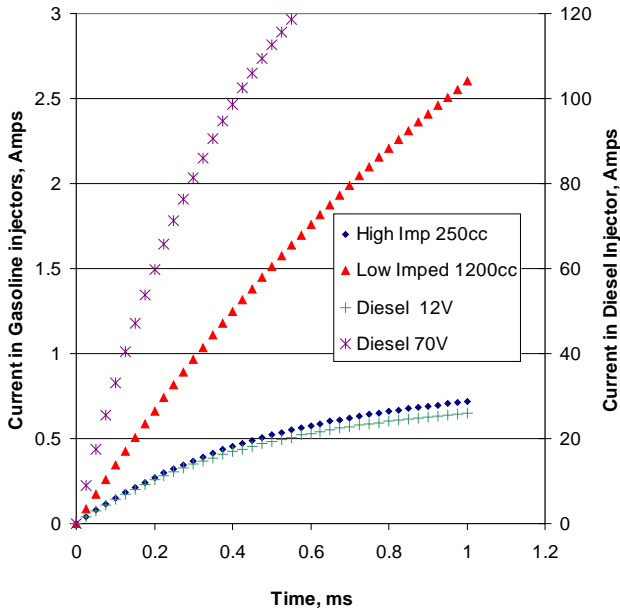


Figure 2. Current increase in the three different injectors with different impedances.

B. Boost Voltage Capacitor Size

Another analytical aspect that was considered before designing and building the switching power circuit for the diesel solenoid valve injectors was the size of capacitor required for the boost voltage. Figure 3 shows the schematic of the idealized circuit to model the capacitor discharge as current in the injector increases. The capacitor is used for the storage of boost voltage generated from the battery 12V by a boost converter, while the inductor and resistor are the internal inductance and internal resistance of the diesel solenoid type injector.

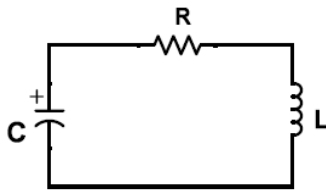


Figure 3. Diagram of supply of injector current from charged capacitor.

Considering the voltage across the inductor and resistor, V

$$L \frac{di}{dt} + iR = V \tag{2}$$

Considering the voltage and charge Q in the capacitor

$$C = \frac{Q}{V} \tag{3}$$

Combining equations 2 and 3

$$L \frac{di}{dt} + iR = \frac{Q}{C} \tag{4}$$

If we consider this from time $t = 0$ when switch is closed to final time t , through discrete steps Δt , we can write

$$L \left(\frac{i_{n+1} - i_n}{\Delta t} \right) + i_n R = \frac{Q_n}{C} \tag{5}$$

$$L(i_{n+1} - i_n) + i_n R \Delta t = \frac{Q_n \Delta t}{C} \tag{6}$$

$$i_{n+1} = \frac{Q_n \Delta t}{CL} - \frac{i_n R \Delta t}{L} + i_n \tag{7}$$

Considering the current and charge in the capacitor

$$i = -\frac{dQ}{dt} \Rightarrow dQ = -idt \tag{8}$$

which can be written in discrete form as

$$Q_{n+1} = Q_n - i_n \Delta t \tag{9}$$

Using equations 7 and 9 a curve of current through the injector and voltage available from the capacitor was plotted. An initial voltage of 70V across the capacitor was used. Iteratively changing the capacitor size it was determined that a 220 μ F capacitor should suffice as the voltage drop is only a few volts in the initial discharge until the 20Amp threshold is reached. Refer to figure 4.

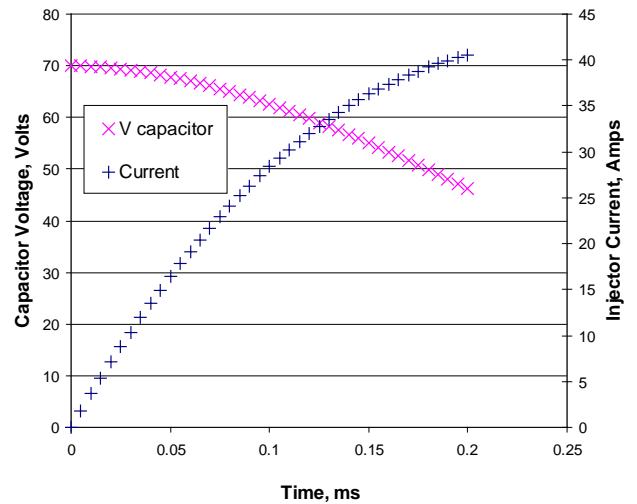


Figure 4. Drop in capacitor voltage against injector current increase using a 220 μ F capacitor.

The injector power switching module comprising the boost converter was built using discrete components. The opening of the diesel injectors was tested in dry mode first, *i.e.* no diesel pressure applied to the injectors. The injectors could be heard to open as injector triggers were imposed.

The peak and hold feature on injector current is shown in the oscilloscope screen shot of figure 5. The upper trace is the current trace measured by an LEM LTS15-NP current sensor while the lower trace is the ECU trigger signal into the

injector power module. It is noted that the initial current increase gradient is steep because it is driven by the 70V boost voltage. During the peak period the injector is driven from the 70 V supply and hence all the current increase slopes are steep while during the hold period the injector is driven from the 12V supply and hence a much lower current increase slope is obtained.

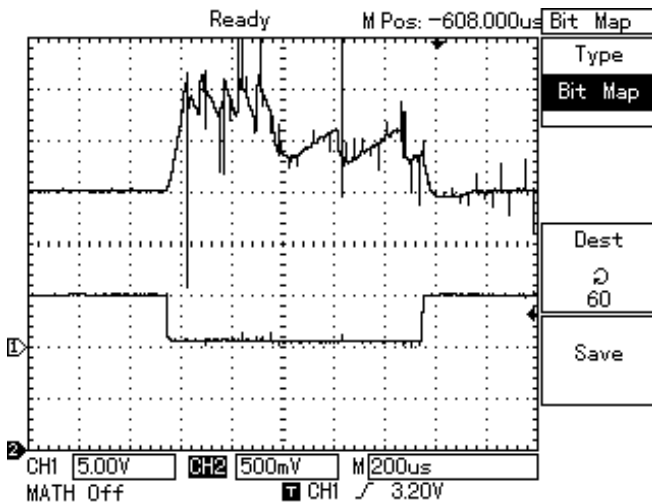


Figure 5. Current in injector (upper trace) and trigger signal (lower trace).

IV. INJECTOR FLOW BENCH TESTING

A fuel injector flow test bench was built. It was composed of the two main fuel pressurization stages as in the vehicle common rail system. These are the high pressure stage and the low pressure stage as shown in figure 6. A low pressure fuel pump was used to deliver fuel from the fuel tank to the high pressure pump. The high pressure pump was toothed-belt driven by a 5kW electric motor. The 5kW motor was speed controlled by means of an inverter. The high pressure fuel pump delivered pressurized fuel to the common rail to which the injectors were connected.

A. 3rd Piston cut-off and Pressure Control solenoids

The Bosch high pressure fuel pump used on the test bench was identical to that used on the engine. The high pressure pump has two electrical control inputs namely the 3rd piston cut-off solenoid and the pressure control solenoid [27]. These two electrically actuated inputs of the pump give flexibility in operation of the supply pressure and flow rate of the pump. The pump has three pistons which pressurize diesel, however the 3rd piston can be electrically deactivated, hence reducing the pump flow rate and consequently the pump shaft power consumption, refer to Figure 7. Using this test bench the functionality and dependency of the fuel pressure within the common rail on the 3rd piston cut-off solenoid and the pressure control solenoid of the Bosch pump were determined. The 3rd piston cut-off was controlled by a manual switch while the duty cycle supplied to the pressure control solenoid was driven by one of the PWM outputs of the ECU. The fuel pressure transducer that is mounted on the common rail to measure fuel rail pressure was connected as an analog signal to the ECU.

Figure 8 shows the variation of pressure in the fuel rail as a function of pressure control solenoid duty cycle. From the figure it can be noticed that neither the 3rd piston cut-off nor the pump speed affect the pressure but pressure is totally controlled by the pressure control solenoid duty cycle. Hence it can be said that both the 3rd piston cut-off and pump speed only affect the pump flowrate capability but not the pressure.

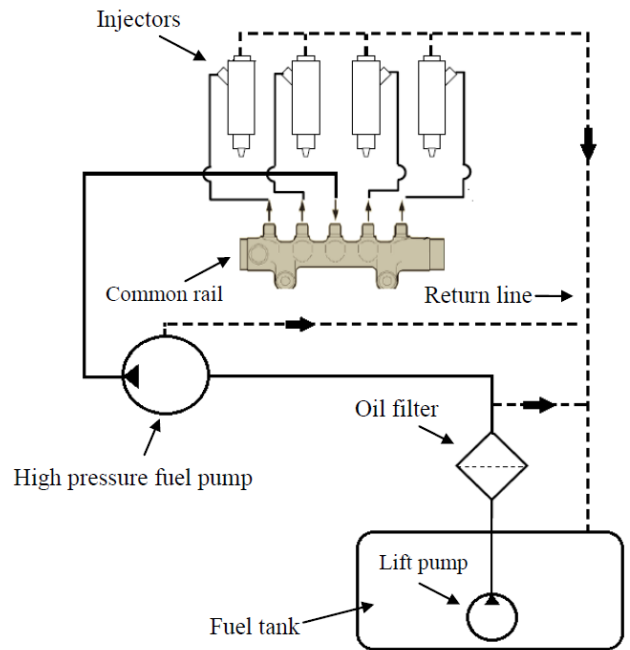


Figure 6. Flow bench schematic of common rail system.

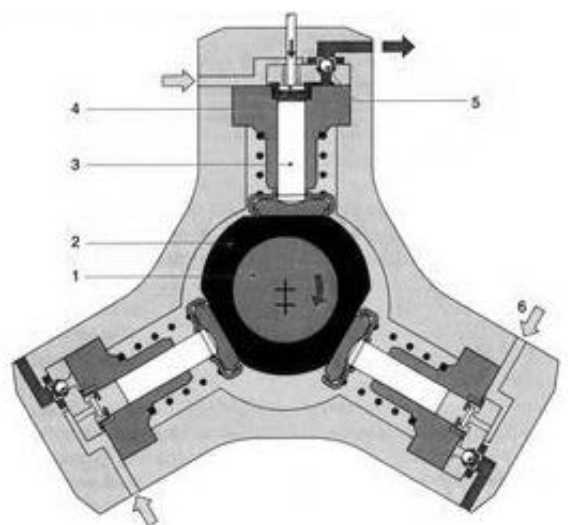


Figure 7. Cross sectional view of high pressure diesel pump[27].

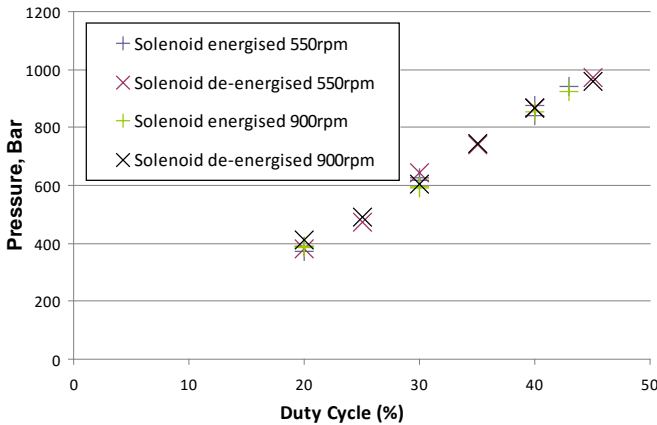


Figure 8. Variation of rail pressure with pressure control solenoid duty cycle.

B. Pressure Control

To further analyze the pressure control of the high pressure pump by means of the Pressure Control Solenoid, it was decided to explore the dependency of the pressure on the duty cycle of PWM control to the solenoid and also the current in the solenoid as a result of the PWM duty cycle. Figure 9 shows the clear linear relationship between the solenoid duty-cycle/current of the solenoid and the pressure. The figure shows that as the duty cycle was increased it resulted in an increase in current and an increase in pressure. The current was analyzed using an LEM LTS6-NP current sensor. It was noted that the current is not ON-OFF, but rather, current is in fact a saw-tooth, increasing during the ON period and decreasing during the OFF period. The current values shown in Figure 9 are the average values. Since current is flowing continuously in the solenoid, it is the opinion of the authors that it is the current quantity that in reality determines the pressure and not the duty cycle. To this effect it was deemed important that the supply voltage to the Pressure Control Solenoid is regulated as discussed in the Section V C below.

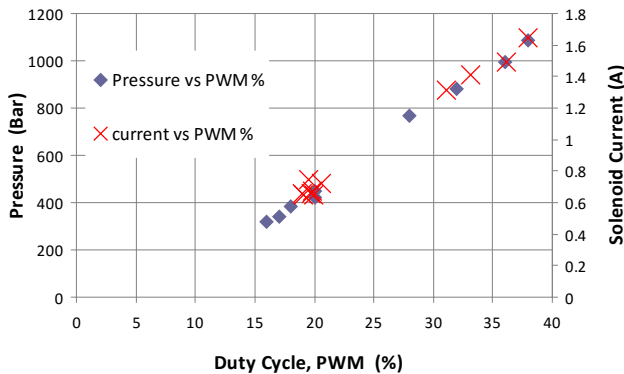


Figure 9. Relationship between the current dissipated and the pressure.

C. Fuel Injector Flow Tests

Apart from providing the capability to test the effects of the 3rd piston cut-off solenoid and the pressure control solenoid, this test bench gave the possibility to test the operation and flowrate of the injectors. Flow tests of the injectors were done at different Duration Of Injection (DOI) and rail pressure as shown in figure 10. It is noted that a linear relationship of flow with DOI was obtained which is similar to gasoline injector operation, e.g. gasoline injector tests detailed in Farrugia [28]. It is noted that in gasoline the fuel flow is controlled by the DOI and the fuel pressure difference from rail to inlet manifold is typically maintained constant by means of a mechanical pressure regulator. Figure 10 shows that fuel pressure effects the flowrate considerably as expected, *i.e.* higher pressures produce higher flow rates.

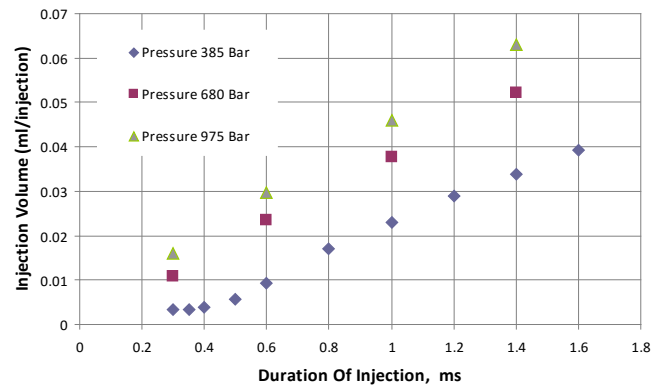


Figure 10. Flow of diesel per injection pulse at different rail pressures.

The flow rate across a restriction or orifice, such as an injector, is a function of the square root of pressure. This can be seen from equation 8 [29].

$$Q = C_d A_t \left[\frac{2(\Delta p)}{\rho (1 - \beta^4)} \right]^{\frac{1}{2}} \quad (8)$$

Where Q is the mass flow rate, C_d is the discharge coefficient, A_t is the area of the throat, Δp is the pressure difference across the nozzle, ρ is the density of the fuel and β is the vena contracta ratio. The data shown in Figure 10 was corrected for pressure to check if the injectors flow did follow a squared root of pressure dependency. Figure 11 shows that the data did collapse and that furthermore it transpired that at low pressures the injectors had an accentuated delay. This delay was deemed to be due to the fact that these diesel injectors are pilot operated driven, that is diesel pressure is used as the motive force to move the heavy internals after the smaller pilot valve is moved electrically.

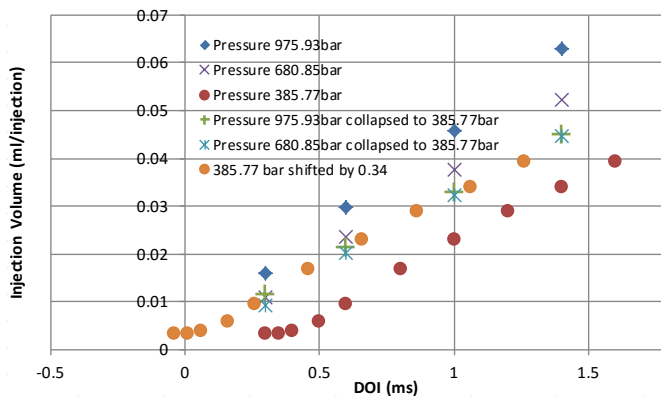


Figure 11. Injector volume vs DOI with 385.77 bar shifted by 0.34ms.

The above results could only be applied when testing the injector on the test bed since Δp is known. It is good to note that for SI engines the Δp across the injector is kept constant by the pressure regulator. In SI the pressure regulator will regulate the pressure in the rail according to the pressure in the intake manifold so that the Δp across the injector is kept constant. On the other hand Δp across the injector for CI engines is not constant since the injection is done inside the cylinder and the pressure in the rail is not a function of the pressure inside the cylinder, whereby pressure would be increased a lot during the compression stroke.

V. DIESEL ENGINE CONTROL SCHEMES

The diesel engine has different requirements than a gasoline engine. However it was preferred to have as much commonality with the gasoline schemes so that ECU development on both versions remains streamlined as much as possible. It was also deemed beneficial if both diesel and gasoline versions are similar so that students and technical people using the two versions of the ECU are able to use both versions concurrently.

The diesel Engine was first tested without load, *i.e.* starting and idle as outlined in Farrugia [26]. Subsequently it was tested in loaded condition on an engine dynamometer as detailed in following sections.

A. Starting and idling control

The ECU and diesel injector power module were connected to the Peugeot diesel engine. The engine was started and made to idle at the desired rpm by imposing a negative gradient of rail pressure with rpm. This idle speed control scheme is in principle the same as that described in Farrugia [28]. Before starting and during cranking the highest possible pressure from the diesel high pressure pump was requested by imposing a very high PWM on the diesel pressure control solenoid. This meant that at low rpm all available pressure was made available to the injector to atomizing the fuel. Therefore the look-up table for the Pressure Control Solenoid output was set to 90% at zero rpm that goes to 12% at 1000 rpm and then to 10% at 5000rpm.

Compensations to fuel quantity and injection timing were still available as for the gasoline case. A starting compensation of 200% (*i.e.* double the table value) for the first 50 revolutions when starting at 20°C engine temperature was found to work. It is noted that the combustion chamber heaters as found on any diesel engine were used and typically 15 seconds of heating was found to be enough when starting at 20°C. Post start, only engine temperature fuel compensation was used which was 120% at 20°C and tapered off to 100% (*i.e.* no extra fuel) at 55°C.

B. Loaded Engine Control

The diesel pressure requirement at high engine speeds and load was required to vary from the idle condition as discussed in the previous section. Initial attempts were to increase rail pressure as a function of rpm, *i.e.* have a control scheme of 90% at zero rpm, goes low to 12 % at 1000rpm, and then starts having an increase of pressure (*i.e.* PWM%) with rpm say goes up to 50% at 2000 rpm and 70% at 5000rpm. This control scheme did not function properly as the engine was able to pick up speed (albeit with some hesitation) on increase of the load parameter input (Torque Request) but the biggest problem was that the engine was not able to get back down in RPM when the Torque Request input was again lowered.

Typically the rail pressure is a function of many parameters not just one but the Reata ECU's configurable PWM outputs are only a function of one selectable parameter. This was considered as a major limitation, but was considered as a challenge worth researching.

In a gasoline engine, the MAF sensor output is a function of both RPM (air mass flow in engine increases with RPM) and throttle opening/boost pressure. Hence MAF is in a way a multiplication of the engine speed (RPM) and load (air-density). In diesel engine this is not exactly the same as the airflow is not affected by throttle opening as typically there isn't any, but it is effected by boost pressure. This means that the MAF sensor in the diesel application still has information from both RPM and boost pressure. Therefore the MAF signal was considered as the best alternative for the control of the Pressure Control Solenoid.

A control scheme based solely on MAF was tested. The look up table implemented increased fuel pressure with MAF to be able to provide the required progressively higher rail pressure with engine speed and load. The zero rpm requirement for maximum pressure was implemented as 90% duty cycle at zero gram per second of air flow. The air flow at idle of around 10 g/s was set to correspond to around 17% duty cycle output to the Pressure Control Solenoid. However engine operation was not satisfactory with less idle quality then when compared to PWM as a function of RPM and the engine was still not able to drop back in speed when Torque Requirement input was brought down as already discussed above.

Therefore the control scheme was further modified to include RPM, MAF and Torque Requirement. This was done through the electrical scheme rather than in programming so

as to maintain as much commonality with the gasoline version as possible.

C. Combining of RPM, MAF and Torque Requirement

As outlined above the Pressure Control Solenoid PWM was found to be optimal if demanding highest pressure at zero rpm and then dropped down to say 10% at 1000rpm to help starting and provide a negative gradient to stabilize engine speed at idle. The MAF requirement was to increase PWM requirement with an increase in air mass flow. Further to the above RPM and MAF dependency, the inclusion of the Torque Requirement was implemented to increase rail pressure when Torque requirement is increased. Therefore Torque Requirement demanded higher pressures from the rail at higher Torque Requirements but would also drop rail pressure when Torque Requirement input was brought down hence directly affecting the engine to drop back in speed (tip out).

As discussed above, the pressure is controlled by current flowing in the Pressure Control Solenoid on the high pressure pump. The current can be varied by PWM control on the ground side and also by the applied voltage on the positive side. Since in an engine operation, the positive side (normally referred to as 12V) is not really a fixed voltage, the current would be effected by the state of the battery voltage. During cranking battery voltage can go down to 9V while charging from the alternator typically brings voltage up to 13.8V. Therefore it was decided to regulate the positive side of the supply to the Pressure Control Solenoid to decouple it from voltage increase due to alternator charging and additionally make it controlled via the Torque Requirement.

Regulation of the positive side was done by an LM317 variable voltage regulator. The output voltage of the LM317 was made to vary as a function of the Torque Requirement by means of a configurable PWM output from the ECU, mosfet Q0 in Figure 12.

The ground side of the Pressure Control Solenoid was duty cycle controlled by means of two PWM outputs from the ECU as a function of RPM and MAF as detailed above. The two PWM outputs were wired together on the drain side of the mosfets to form an OR of the two outputs as shown in Figure 13. The mosfet outputs could be wired together to form an OR function since the ECU was outputting these two PWM outputs synchronously and in-phase with one another as shown in Figure 14. It is noted that the mosfet is ON when the voltage is low and therefore the Pressure Control Solenoid is energized when any of the two mosfets is switched to ground. The screen shot of Figure 14 shows the two PWM outputs, upper trace is MAF output, while lower trace is RPM output. In the shown condition, zero RPM and zero MAF, the respective duty cycles are 80% and 15%. The complete list of PWM values as a function of RPM, MAF and Torque Requirement are given in Tables II, III and IV respectively. The stated values in the tables were the final values found to give optimal engine response. Table IV shown the % PWM output as a function of the Torque Requirement signal input and gives also the resulting voltage output from the variable voltage regulator LM317.

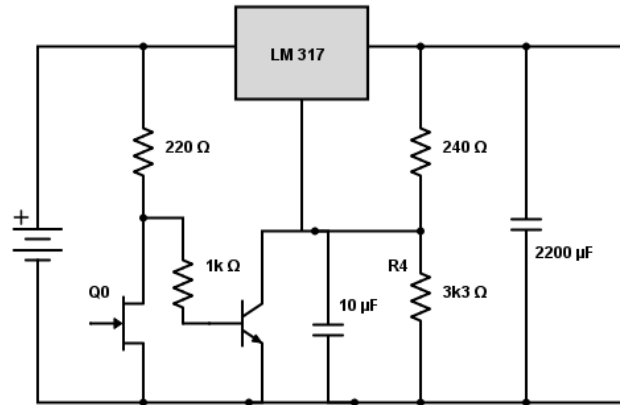


Figure 12. Schematic of the voltage regulation as a function of the Torque Requirement.

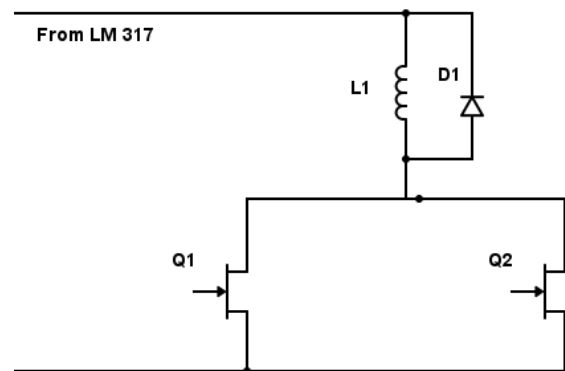


Figure 13. Pressure Control Solenoid (L1) controlled by OR of the two PWM outputs that are a function of RPM (Q1) and MAF (Q2).

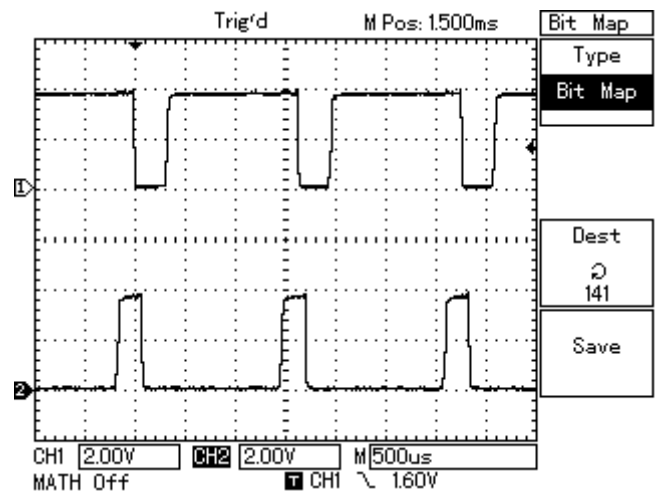


Figure 14. Oscilloscope screenshot of the two PWM outputs that are a function of RPM and MAF.

The look up tables that were found to provide good control of the fuel pressure are the following.

TABLE II. RPM PWM OUTPUT LOOK UP TABLE

<i>RPM</i>	<i>PWM % Output</i>
0	80
1000	12
5000	10

TABLE III. MASS AIR FLOW PWM OUTPUT LOOK UP TABLE

<i>Mass Air Flow MAF</i>	<i>PWM % output</i>
0	15
10	26
20	30
30	30
35	35
40	35
45	40
50	45
60	50
70	60
160	70

TABLE IV. TORQUE REQUIREMENT PWM OUTPUT LOOK UP TABLE, AND RESULTING LM317 VOLTAGE OUTPUT

<i>Torque Requirement</i>	<i>PWM % Output</i>	<i>Output Voltage V</i>
0	0	5.4
20	50	9.1
40	50	9.1
50	70	11.2
60	90	12.4
95	100	12.4

D. Adaption of Speed Density Control

In gasoline engines the speed-density control strategy is very effective and popular. The speed is the RPM, while the density is probably better referred to as load. In gasoline engine the load is varied by throttling the incoming air and hence the density of the incoming air. The air density in a gasoline engine relates directly to the amount of fuel that can be injected to maintain an air to fuel ratio close to stoichiometric. In diesel engines the load is controlled by the

quantity of the fuel that is injected. The driver's request/wish, or accelerator pedal position is referred to as Torque Requirement. The term Torque Requirement is a generic term that can be used also on drive by wire gasoline engines where the throttle body is not mechanically directly controlled by the accelerator pedal but is electronically driven.

The Fuel Map is a table which specifies the Duration Of Injection of the injectors for RPM vs Torque Requirement. As discussed previously the actual flow that flows out of the injectors is not only a function of the Duration Of Injection but also a function of rail pressure. The initial Fuel Map was populated by engineered choices as a start. Experimental testing on a water brake dynamometer in steady-state was then conducted to determine optimal values for the loaded conditions. The 90% Torque Requirement column was chosen at a fuel quantity which does generate a quantity of smoke (can be regarded as our chosen smoke limit, also refer to Obert [30] page 344 for Bosch Smoke Number). The 70% column does not generate any smoke. The 50% column was chosen to generate approximately 50% of the torque produced at 90%. While the 5% is the idle (no load) condition. The fuel Map is given in Table V.

The injection timing table was found experimentally to produce the best torque at the respective cells. The injection timing specifies the crank angle before top-dead-centre at which the ECU triggers the injector to inject fuel. The injection map is given in Table VI.

TABLE V. FUEL QUANTITY TABLE, MILLISECONDS

<i>RPMt</i>	<i>Torque Requirement</i>				
	<i>5</i>	<i>20</i>	<i>50</i>	<i>70</i>	<i>90</i>
0	1.200	1.00	1.00	1.20	1.40
500	0.99	0.70	0.80	1.00	1.30
1000	0.60	0.80	1.15	1.25	1.55
1500	0.41	0.70	0.91	1.21	1.50
2000	0.30	0.65	0.71	1.08	1.44
2500	0.25	0.45	0.51	1.00	1.50
3000	0.20	0.40	0.50	0.93	1.35
3500	0.10	0.38	0.47	0.79	1.10
4000	0.10	0.35	0.43	0.77	1.10

TABLE VI. INJECTION TIMING TABLE, CRANK ANGLE BEFORE TOP DEAD CENTRE

RPM	Torque Requirement				
	5	20	50	70	90
0	15	15	15	15	15
500	15	15	15	15	15
1000	15	12	20	15	15
1500	15	15	21	20	14
2000	10	15	21	20	14
2500	10	15	23	22	21
3000	12	15	24	25	25
3500	12	17	24	24	28
4000	15	17	23	25	28

The engine torque and power output is shown in Figure 15. This experimental data was obtained from a curve fit of the points produced during a pull on the engine dynamometer, *i.e.* it is not from steady state testing.

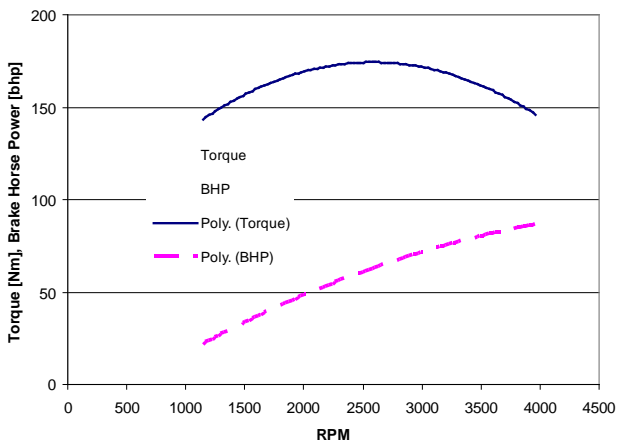


Figure 15. Torque and Power Output of the controlled diesel engine.

E. 3rd Piston Cutoff Solenoid Valve

The 3rd Piston Cutoff valve was found to be not critical for proper engine operation. Tests showed that the pressure in the rail was only a function of the Pressure Control Solenoid and not effected by the 3rd Piston. Comparison of rail pressure during engine dynamometer pulls showed that the pressure was slightly lower when operating on two pistons rather than three. , However comparison of the torque (and hence also power) output was practically the same with either the 3rd piston activated or not.

VI. CONCLUSION

A control strategy for the control of a common rail diesel engine was detailed in this work. The ECU used is an evolution of a programmable gasoline ECU. The control scheme is an extension of the speed-density system which is very popular for control of gasoline engines. A scheme for the control of the common rail pressure based mostly on the Mass Air Flow sensor was experimentally tested and found to be very effective. Diesel injector flow rate data as a function of duration of injection and rail pressure is also given. Optimized fuel quantity and injection timing maps from loaded engine experiments on the dynamometer are given. The discussed diesel engine setup controlled by the programmable ECU was developed to empower the thermodynamics laboratory for research into dual fuel systems, Diesel Particulate Filter loading, and other diesel engine related concepts.

ACKNOWLEDGMENT

Mr Andrew Briffa and Ing Noel Balzan are thanked for their assistance in this project. Mr Jean Paul Azzopardi is acknowledged for his idea to use MAF sensor as the main control parameter for the Pressure Control Solenoid control of rail pressure. The support of the University of Malta Research Fund is also acknowledged.

REFERENCES

- [1] Oudghiri M., Chadli M., and El Hajjaji A., "Robust Fuzzy Sliding Mode Control For Antilock Braking System", Int Journal on Sciences and Techniques of Automatic control Vol. 1, No1., June 2007.
- [2] Hagen, D., "Electronic engine controls at Ford Motor Company," SAE Technical Paper 780842, 1978, doi:10.4271/780842.
- [3] Breitzman, Richard C., "Development of a Custom Microprocessor for Automotive Control", IEEE Control Systems Magazine, May 1985
- [4] Gerhardt, J., Hönninger, H., and Bischof, H., "A New Approach to Functional and Software Structure for Engine Management Systems - BOSCH ME7," SAE Technical Paper 980801, 1998, doi:10.4271/980801.
- [5] Peyton Jones, J. and Muske, K., "Automatic Calibration of 1 and 2-D Look-up Tables using Recursive Least-squares Identification Techniques," SAE Technical Paper 2007-01-1343, 2007, doi:10.4271/2007-01-1343
- [6] Qian Weikang , "Practical solution for automotive electronic throttle control based on FPGA", Signal Processing, ICSP. 9th International Conference Oct. 2008
- [7] Ishmael Zibani, Joseph Chuma and Rapelang Marumo, "Designing a model of a full control module for a camless engine employing rotary valves", AFRICON, 2013 Date 9-12 Sept. 2013, DOI 10.1109/AFRCON.2013.6757724, IEEE Computer Society
- [8] Jakob Axelsson, "HW/SW Codesign for Automotive Applications: Challenges on the Architecture Level", Proceedings of the Fourth International Symposium on Object-Oriented Real-Time Distributed Computing (ISORC'01) 0-7695-1089-2/01 IEEE 2001.
- [9] Tahat, A., Said, A., Jaouni, F., & Qadamani, W. (2012, June). Android-based universal vehicle diagnostic and tracking system. In Consumer Electronics (ISCE), 2012 IEEE 16th International Symposium on (pp. 137-143). IEEE.

- [10] Sáinz *et al.* (2011). Conversion of a gasoline engine-generator set to a bi-fuel (hydrogen/gasoline) electronic fuel-injected power unit. *international journal of hydrogen energy*, 36(21), 13781-13792.
- [11] de Oliveira, A., dos Santos, E. C. M., Botelho, G. C., Valente, O. S., & Sodré, J. R. (2013). Hydrogen electronic injection system for a diesel power generator. *International Journal of Hydrogen Energy*, 38(19), 7986-7993.
- [12] Ergenç, Alp Tekin, and Deniz Özde Koca. "PLC controlled single cylinder diesel-LPG engine." *Fuel* 130 (2014): 273-278.
- [13] Wierzbicki, Sławomir, Michał Śmieja, and Andrzej Pięta. "Preliminary tests on an integrated laboratory control system for the feeding system of a dual-fuel diesel engine and its load." *Journal of KONES* 20 (2013).
- [14] Gu, Xiaolei, Guo Li, Xue Jiang, Zuohua Huang, and Chia-fon Lee. "Experimental study on the performance of and emissions from a low-speed light-duty diesel engine fueled with n-butanol–diesel and isobutanol–diesel blends." *Proceedings of the Institution of Mechanical Engineers, Part D: Journal of Automobile Engineering* 227.2 (2013): 261-271.
- [15] Tschanz, Frédéric, Alois Amstutz, Christopher H. Onder, and Lino Guzzella. "Feedback control of particulate matter and nitrogen oxide emissions in diesel engines." *Control engineering practice* 21, no. 12 (2013): 1809-1820.
- [16] Giordani Andreoli, Alexandre, Fabricio Da Silva Stein, and Carlos E. Pereira. "Development of an electronic management system for a rotary combustion engine." In *Industrial Informatics (INDIN)*, 2014 12th IEEE International Conference on, pp. 140-146. IEEE, 2014.
- [17] Powell, J. David, N. P. Fekete, and Chen-Fang Chang. "Observer-based air fuel ratio control." *Control Systems, IEEE* 18, no. 5 (1998): 72-83.
- [18] Wong, Pak Kin, Hang Cheong Wong, Chi Man Vong, Zhengchao Xie, and Shaojia Huang. "Model predictive engine air-ratio control using online sequential extreme learning machine." *Neural Computing and Applications* (2014): 1-14.
- [19] Hiticas, I, Marin, D., L. Mihon, E. Resiga, and D. Iorga. "Parameters control of a spark ignition engine through programmable ECU for specific regimes." In *Applied Computational Intelligence and Informatics (SACI)*, 2012 7th IEEE International Symposium on, pp. 399-404. IEEE, 2012.
- [20] Farrugia, Mario; Rossey, Mike; Sangeorzan, Brian; "ECU Development for a Formula SAE Engine", SAE Paper 2005-01-0027. SAE World Congress April 11-14, 2005. DOI 10.4271/2005-01-0027
- [21] Farrugia, Mario; Grech, Nicholas; Chirchop, Marlon; Azzopardi, JeanPaul; "Simulation and Implementation of Turbocharging a 600cc Engine for FSAE", 20th International Conference Engineering Mechanics 2014, Svratka Czech Republic, May 2014
- [22] Zammit, Glenn; Farrugia, Mario; Ghirlando, Robert; Bachmann, Chris; "Experimental investigation of the effects of hydrogen enhanced combustion in SI and CI engines on performance and emissions", HEFAT 2012, 9th International Conference on Heat Transfer, Fluid Mechanics and Thermodynamics, Malta, 16-18 July 2012.
- [23] Busuttill, Daniel; Camilleri, Glenn; Farrugia, Mario; "Mechatronics for Water Injection in SI Engine", Proceedings of the 16th International Conference on Mechatronics –Mechatronika 2014, 3-5 December 2014 BRNO Czech Republic.
- [24] Busuttill, Daniel; Farrugia, Mario; "Experimental Investigation on the Effect of Injecting Water to the Air to Fuel Mixture in a Spark Ignition Engine", MM (Modern Machinery) Science Journal, March 2015, p585-590. ISSN 1805-0476.
- [25] Farrugia, Mario; Briffa, Andrew; Farrugia, Michael; "Liquid State LPG Conversion of an Older Vehicle", SAE International Powertrain Fuels and Lubricants Conference, 20-23 October Birmingham UK, SAE Paper 2014-01-2613, DOI 10.4271/2014-01-2613.
- [26] Farrugia Mario, Seychell Charlo, Camilleri Stephen, Farrugia Gilbert, and Farrugia Michael, "Development of a Programmable Engine Control Unit to Multi-FuelCapabilities, Progression to Diesel", 16th international conference on Sciences and Techniques of Automatic control & computer engineering - STA'2015, Monastir, Tunisia, December 21-23, 2015.
- [27] Robert Bosch GmbH, Diesel-Engine Management 4th Edition, Wiley 2005, pg282-297, ISBN 0-470-02689-8.
- [28] Farrugia, Mario; Rossey, Mike; Sangeorzan, Brian P; "On the use of a Honda 600cc 4-Cylinder Engine for Formula SAE Competition", SAE Paper 2005-01-0025. SAE World Congress April 11-14, 2005. DOI 10.4271/2005-01-0025
- [29] F. M. White, "Viscous Flow in Ducts," in *Fluid Mechanics*, New York, McGraw-Hill, 2011, pp. 398-399,
- [30] Obert E. and Jennings B., , Exhaust gas analysis and air pollution pp.344 in "Internal combustion engines", Scranton: International Textbook Co, 1968, ISBN 700221832.